Proceedings of the 24th European Young Geotechnical Engineers Conference (EYGEC), Durham, UK
Osman, A.S. & Toll, D.G. (Eds.) 2015
ISBN 978-0-9933836-01

Dilatancy Based Calculation of Passive Earth Thrust and the Locked-in Stress Concept

Ahmet Talha Gezgin[1] and Ozer Cinicioglu[1]

[1] *Bogazici University, Istanbul, Turkey*

ABSTRACT Magnitude of earth thrust acting on retaining structures at the instance of passive failure is dependent on the strength of the soil body and the geometry of the resulting failure surface. Accordingly in this study, a new method for the calculation of passive earth thrust is proposed. For this purpose, a new equation (Altunbas 2014) that provides dilatancy based determination of the geometry of the passive failure plane is incorporated into the method of slices for the calculation of passive earth thrust. Accuracy of the proposed method is verified using the results obtained from small-scale physical retaining wall model tests. Comparing the calculated and measured passive thrust magnitudes, it was noticed that the results were different for the model tests with compacted backfills, whereas they were compatible for the model tests with pluviated backfills. The reasons for the differences are discussed theoretically and quantitatively. Hence, a new concept called locked-in stresses is developed to consider elastically stored residual normal stresses in soil bodies and their influences on strength.

1 INTRODUCTION

Correct calculation of the lateral earth forces is critical in the design of geotechnical structures that retain soil.

Preliminary studies on ultimate lateral earth pressures assumed planar failure surfaces (Rankine 1857, Coloumb 1776). According to these theories, passive earth pressure coefficient is basically a function of internal friction angle and backfill-wall interface friction angle. As a result, theoretically assumed failure surfaces are significantly different than real ones, resulting in computed pressure magnitudes that deviate from measured values. Noticing this defect, several researchers proposed parabolic and curvilinear failure surfaces (Terzaghi 1943, Handy 1985, Harrop-Williams 1989, Wang 2000, Paik and Salgado 2003, Goel and Patra 2008). Moreover, in order to adopt a more precise method for calculations, some researchers have concentrated on the generalized method of slices to solve lateral earth thrust problems using composite failure surface (Janbu 1957, Shields and Tolunay 1972, Rahardjo 1982 and Zakerzadeh 1999). The common shortcoming of all these studies is that the failure surface geometries that were proposed were not directly dependent on the soil properties, thus they do not reflect backfill-specific behavior. To address this deficiency, Altunbas et al. (2014) proposed a new approach to the definition of failure planes based on backfill dilatancy angle. Accordingly, this study assumes the dilatancy based failure surface geometry proposed by Altunbas et al. (2014) and attempts to calculate passive thrust by adopting the method of slices (Rahardjo 1982, Zakerzadeh 1999) approach to lateral earth force problems.

Accuracy of the developed method was evaluated through small scale retaining wall model tests. Comparison of model test results and calculated values revealed that passive earth thrust is also dependent on the method of backfill preparation. The influence of backfill preparation method is quantified using a new concept called “locked-in stresses”. Finally, the results are discussed and the proposed method is compared with popular methods for calculating passive earth pressures.

2 TEST SETUP

A small scale retaining wall model (Figure 1) setup that allows the measurement of lateral earth pressures was designed and manufactured in Karl Terzaghi Soil Mechanics Laboratory at Bogazici University. The model consists of a testing tank, retaining wall, high sensitive pressure transducers, sand pluviation sys-

tem, storage tank, crane and multi-channel data logger. Sides of the testing tank are plexiglass allowing the observation of deformations during testing. An aluminum plate capable of lateral translation works as a retaining wall and simulates active and passive deformations states. The wall has a rectangular cross-section that is 35 cm high and 120 cm long. In order to minimize the adverse effects of the rigid boundary at the bottom, the moving plate that simulates the vertical retaining wall is located 15 cm above the bottom of the test box. There are five sensitive pressure transducers mounted on the retaining wall model. These transducers allow the measurement of lateral earth pressures acting on the wall.

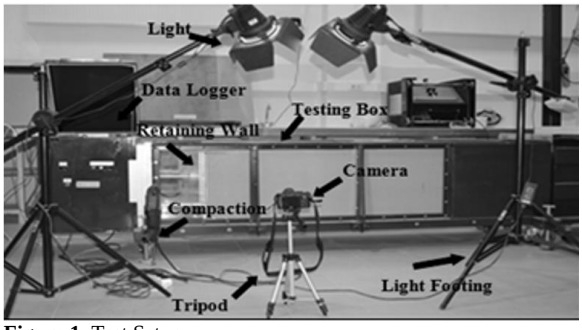

Figure 1. Test Setup.

3 CALCULATION OF PASSIVE EARTH THRUST USING METHOD OF SLICES

Geometry of the failure surface as a function of the backfill dilatancy angle is identified using the equation proposed by Altunbas (2014). The soil mass above this surface is divided into thin slices with equal widths. Forces that are assumed to act on each slice are illustrated in Figure 2. Satisfying the equations of equilibrium, forces acting on each slice are identified. Additionally, magnitudes of the shear forces mobilized on the base of each slice are calculated in accordance with the Mohr-Coulomb failure criterion.

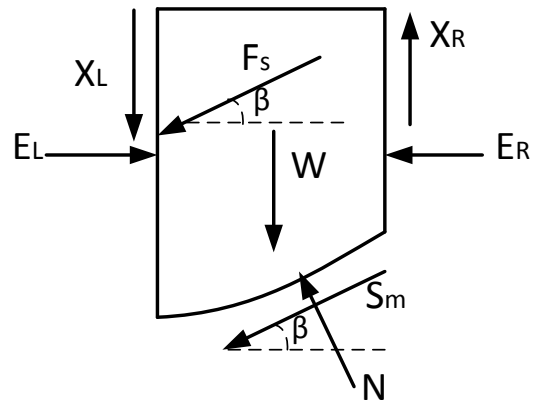

Figure 2. Forces acting on each slice.

In Figure 2, W = weight of the slice, N = normal force on the base of the slice, S_m = shear force on the base of the slice, F_s = friction angle between the backfill and the plexiglass surface, E_L = the horizontal normal interslice forces on the left side, E_R = the horizontal normal interslice forces on the right side, X_L = The vertical shear interslice forces on the left side, X_R = The vertical shear interslice forces on the right side and β = The angle between the tangent to the center of the base of the slice and the horizontal.

The relationship between shear and normal interslice forces are assumed to conform to the proposition of Zakerzadeh (1999) as given by Eq. [1].

$$\frac{X}{E} = -\left(tan\delta\right) \times \frac{x}{L} \qquad [1]$$

where: δ = backfill-wall interface friction angle, L = horizontal distance between the wall and the point at which the failure surface emerges at the backfill surface (reference point), x = the distance from the reference point to the midpoint of the slice. It is seen that the ratio of interslice shear force to interslice normal force varies with the distance between the wall and midpoint of each slice. The horizontal length along the failure surface (L) and the distance from the wall to the midpoint of the slice (x) are shown in Figure 3.

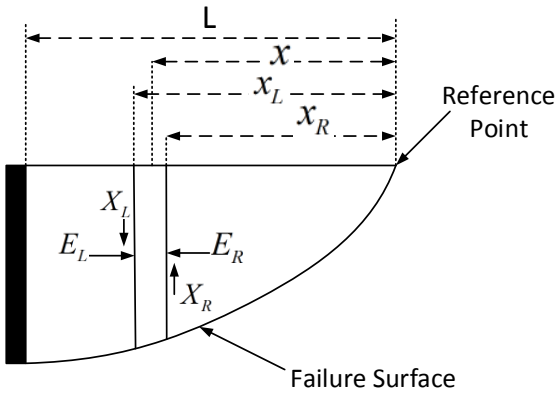

Figure 3. The length from the starting point of the failure surface to a desired point on the failure surface.

In order to calculate the normal force acting on the base of a slice, equilibrium equations are written for both horizontal and vertical directions and rearranged to yield N as shown in Eq. [2].

$$N = \frac{\left(F_s \times \left(\sin\beta - \frac{\cos\beta \times \tan\delta \times x}{L}\right) + W\right)}{\left(\cos\beta - tan\phi' \times sin\beta + \frac{\tan\delta \times x \times \left(\sin\beta + tan\phi' \times \cos\beta\right)}{L}\right)} \quad [2]$$

Within this study, the aim is to describe normal forces as functions of backfill dilatancy angle. Dilatancy angle is calculated using the equation proposed by Cinicioglu and Abadkon (2015) that is based on the relative density and confining pressure of the backfill. Even though in Eq.[2] backfill dilatancy angle does not emerge as an independent parameter, the angle β (Figure 2) and the horizontal length L (Figure 3) are described in terms of backfill dilatancy angle as explained in detail by Gezgin (2015). Therefore, the normal force can be is calculated as a function of dilatancy angle using Eq. [2].

The magnitude of passive earth thrust acting on the wall, P_p, can be computed from the overall equilibrium of forces in the horizontal direction:

$$P_p = \frac{\Sigma\left(N \times sin\beta\right) + \Sigma\left(S_m \times cos\beta\right) + \Sigma\left(F_S \times cos\beta\right)}{cos\delta} \quad [3]$$

4 THE RESULTS

Using the proposed method, passive earth thrust magnitudes are computed for the backfills of model tests. Computed passive thrust magnitudes were compared with the measured ones. The results are shown in Figure 4.

Figure 4. Comparison of the computed and measured passive thrust magnitudes.

When Figure 4 is studied, it is noticed that the computed results are compatible with the measured ones for the tests which have pluviated backfills. On the other hand, for model tests that have compacted backfills, computed and measured results were significantly different. This difference will be carefully investigated in the following section.

5 LOCKED-IN STRESS CONCEPT

Pluviated samples' grains are not exposed to any significant elastic deformation. Therefore, each grain finds a suitable position within the soil skeleton as shown Figure 5(a). However, in cases where vibration plus force is applied, grains are forced into small intergranular voids present in the soil skeleton. This mechanism results in the elastical deformation of grains as illustrated in Figure 5(b).

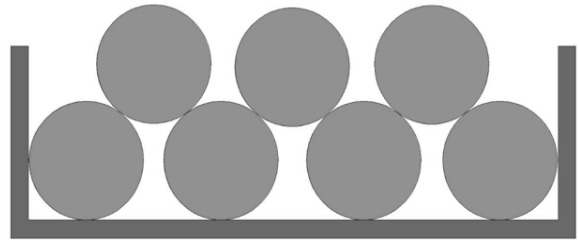

(a)

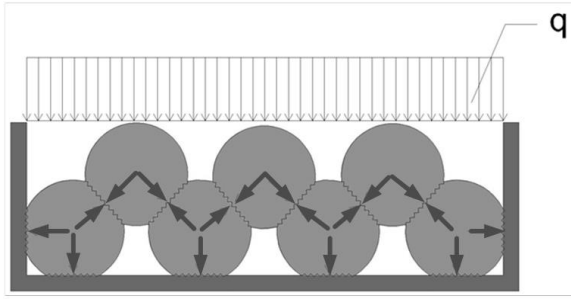

(b)

Figure 5. Soil particles in a tank a) before the compaction b) after the compaction (deformations are exaggerated for clarity).

Elastic deformation of grains is similar to the compression of elastic springs. The grains attempt to return back to their original shapes, thus applying intergranular forces at the points of contact. Resulting additional intergranular normal forces increase the effective stresses above the value that is computed based on the unit weights of the overlying materials. Hence, for frictional materials, increase in effective stresses results in increased strength. Moreover, elastic deformation of the soil particles leads to an increase in the magnitude of coefficient of lateral earth pressure at rest (K_o). Since these elastic deformations are similar to compressed springs increasing the normal stresses within the skeleton, they are referred to as locked-in stresses.

The magnitude of locked-in stresses should be equal to the difference of mean effective stresses at the compacted state and pluviated (normally compressed) state. Thus, locked-in stresses (l_σ) can be computed using Eq. [4].

$$l_\sigma = ((p_i^{'})_{comp} - (p_i^{'})_{nc}) \quad [4]$$

where: $(p_i^{'})_{comp}$ = initial mean effective stress in compacted cohesionless soil, $(p_i^{'})_{nc}$ = initial mean effective stress in normally-compressed cohesionless soil.

Mean effective stresses at the pluviated state and compacted state are calculated using Eq.[5] and Eq. [6], respectively.

$$(p_i^{'})_{nc} = \frac{(\sigma_v^{'})_{nc} + 2\times(\sigma_h^{'})_{nc}}{3} = \frac{(\sigma_v^{'})_{nc}\times(1+2\times(K_o)_{nc})}{3} \quad [5]$$

$$(p_i^{'})_{comp} = \frac{(\sigma_v^{'})_{comp} + 2\times(\sigma_h^{'})_{comp}}{3} = \frac{(\sigma_v^{'})_{comp}\times(1+2\times(K_o)_{comp})}{3} \quad [6]$$

where: $(\sigma'_v)_{nc}$ = effective vertical stress in uncompacted cohesionless soils, $(\sigma'_v)_{comp}$ = effective vertical stress in compacted cohesionless soils, $(\sigma'_h)_{nc}$ = effective horizontal stress in uncompacted cohesionless soils, $(\sigma'_h)_{comp}$ = effective horizontal stress in compacted cohesionless soils, $(K_o)_{nc}$ = lateral earth pressure coefficient at rest in uncompacted cohesionless soils and $(K_o)_{comp}$ = lateral earth pressure coefficient at rest in compacted cohesionless soils.

Locked-in stresses result in higher confinement in cohesionless soils. For this reason, the influence of locked-in stresses on strength is similar to cohesion effect. Additional normal stress mobilizes friction. Thus, one has to account for an additional strength component that is equal to locked-in stress times tangent of peak friction angle. The extra strength can be added to the strength dependent on normal confinement. This extra strength can be calculated using Eq. [7].

$$S_m = (S\times l_\sigma + N)\times tan\phi_p^{'} \quad [7]$$

where: S = length of the base of the a slice, I_σ = locked-in stress at base of a slice, ϕ'_p= peak internal friction angle. Peak internal friction angle (ϕ'_p) is calculated from the relative density and confining pressure of the backfill (Cinicioglu and Abadkon, 2015).

The method proposed for the calculation of passive earth thrust is modified considering the influence of locked-in stresses (Eq. [8]).

$$N = \frac{\left(\left(F_s + l_\sigma\times\tan\phi_p^{'}\times S\right)\times\left(\sin\beta - \frac{\cos\beta\times\tan\delta\times x}{L}\right) + W\right)}{\left(\cos\beta - tan\phi_p^{'}\times sin\beta + \frac{\tan\delta\times x\times(\sin\beta + tan\phi_p^{'}\times\cos\beta)}{L}\right)} \quad [8]$$

The strength that results from locked-in stresses does not have an effect on only normal forces acting at base of all the slices, but also passive lateral earth thrusts acting on the wall directly. Eq. [3] is modified to calculate passive lateral earth thrusts that include effect of locked-in stresses using Eq.[9].

$$S_m = \left(S \times l_\sigma + N\right) \times tan\phi_p^{'} \qquad [9]$$

6 PASSIVE THRUST CALCULATED CONSIDERING LOCKED-IN STRESSES

Passive thrust magnitudes calculated by considering the locked-in stresses are compared with the measured values from the small scale retaining wall model tests. Additionally, both values are compared with the passive thrust magnitudes calculated using the popular lateral earth pressure theories of Rankine (1857) and Coulomb (1776). All the comparisons are shown in Figure 6 and Figure 7.

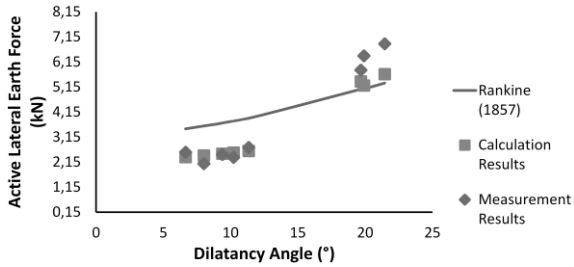

Figure 6. The relationship between dilatancy angle and passive lateral earth thrust according to calculation results, measurement results and Rankine theory.

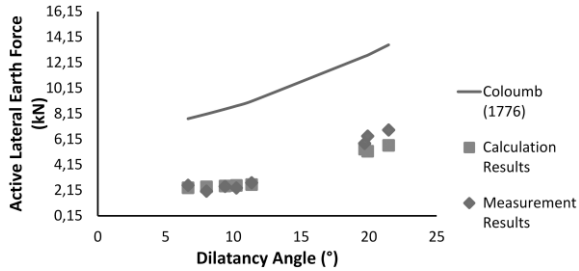

Figure 7. The relationship between dilatancy angle and passive lateral earth thrust according to calculation results, measurement results and Coulomb theory.

7 CONCLUSION

This study attempts to quantify passive lateral earth thrust using realistic failure surface geometry and strength parameters. Realistic failure surface geometries are calculated as functions of peak dilatancy angle using the equation proposed by Altunbas (2014). Peak friction and peak dilatancy angles are calculated as functions of relative density and confining pressure (Cinicioglu and Abadkon 2015).

Defined failure surfaces are incorporated into conventional slice methods (Gezgin 2014). Resulting equations were used to compute ultimate earth thrusts.

Model tests were conducted to test the accuracy of the proposed method. As a result of comparison between the calculated and measured results, it has been observed that knowledge of realistic failure surface geometries and strength parameters are not sufficient for correct calculation of compacted soils, whereas there is good agreement between calculated and measured thrust magnitudes for pluviated backfills. This difference between pluviated and compacted backfills is explained by identifying the influence of work done during compaction for elastically deforming the soil grains. Elastic deformation of grains causes an increase in the intergranular stresses. These additional stresses are referred to as locked-in stresses.

When locked-in stresses are considered, compatibility between the calculated and measurement results has been achieved for the tests with compacted backfills. As a result, it is concluded that, in any design calculation concerning compacted soils, locked-in stresses should be considered for achieving greater accuracy.

ACKNOWLEDGEMENT

The authors would like to thank The Scientific and Research Council of Turkey (TUBITAK) for supporting this study with Project number 110M595.

REFERENCES

Altunbaş, A. Soltanbeigi, B. ve Çinicioğlu, Ö. 2014. Kohezyonsuz Dolguların Aktif Göçme Durumunda Oluşan Kayma Yüzeylerinin Tanmlanması. *Zemin Mekaniği ve Temel Mühendisliği 15. Ulusal Kongresi*, Ankara.

Altunbaş, A.. 2014. Influence of Dilatancy on Slip Planes and on Localization of Strains. Ph.D. Dissertation, Boğaziçi University.

Cinicioglu, O. and Abadkon, A. 2015. Dilatancy and Friction Angles Based on In Situ Soil Conditions. *J. Geotech. Geoenviron. Eng.*, 141(4), 06014019.

Coulomb, C. A. 1776. Essai Sur Une Application Des Regles de Maximis et Minimis`a Quelques Probl`emes de Statique, *Relatifs `a l'Architecture, Memoires de l'Academie Royale Pres Divers Savants* **3**, 343-382.

Fredlund, D. G. Krahn, J. and Pufahl, D. E. 1981. The relationship between limit equilibrium slope stability methods. *In Proceedings of the International Conference on Soil Mechanics and Foundation Engineering*, Stockholm, Sweden, **3**, 409–416.

Gezgin, A. T. and Cinicioglu O. 2014. Aktif Zemin İtkisinin Genleşim Açısına Bağlı Hesaplanması. *Zemin Mekaniği ve Temel Mühendisliği Onbeşinci Ulusal Kongresi*, Ankara.

Gezgin, A. T. 2015. Dilatancy Based Calculation of Lateral Earth Thrust and the Locked-in Stress Concept. M.Sc. Dissertation, Boğaziçi University.

Goel, S. and Patra, N. R. 2008. Effect of arching on active earth pressure for rigid retaining walls considering translation mode. *Int. J. Geomech.* **8**-2, 123–133.

Handy, R. L. 1985. The arch in soil arching. *J. Geotech. Engng.* **111**-3, 302–318.

Harrop-Williams, K. 1989. Geostatic wall pressures. *J. Geotech. Engng.* **115**-9, 1321–1325.

Janbu, N. 1957. Earth Pressure and Bearing Capacity Calculations by Generalized Procedure of Slices. *Proceedings, 4th Int. Conf. on Soil Mechanics and Foundations Engineering*, London, 2, 207-212.

Paik, K. H. and Salgado, R. 2003. Estimation of active earth pressure against rigid retaining walls considering arching effects. *Ge´otechnique.* **53**-7, 643–653.

Rahardjo, H. and Fredlund, D. G. 1984. General limit equilibrium method for lateral earth force. *Canadian Geotechnical Journal*, **21**, 166–175.

Rankine, W. M. J. 1857. On Stability on Loose Earth. *Philisophic Transactions of Royal Society*, London, **I**, 9-27.

Terzaghi, K. 1943. *Theoretical soil mechanics*. Wiley, New York.

Terzaghi, K. and Peck, R. B. 1967. *Soil Mechanics in Engineering Practice, 2nd Ed*., Wiley, New York.

Shields, D. H. and Tolunay, Z. A. 1973. Passive pressure coefficients by method of slices. *Journal of the Soil Mechanics and Foundations Division, ASCE*, **99-12**, 1043–1053.

Wang, Y. Z. 2000. Distribution of earth pressure on a retaining wall. *Geotechnique.* 50-1, 83-88.

Zakerzadeh , N. Pufahl, D. E. and Fredlund, D. G. 1999. Suitable Interslice Force Functions to Solve Lateral Earth Force Problems. *Proceedings of the Eleventh Pan American Conference on Soil Mechanics and geotechnical Engineering*, Iguanzu Falls, Brazil, **3,** 1297-1304.